Am J Cancer Res 2023;13(11):5626-5640
www.ajcr.us /ISSN:2156-6976/ajcr0150452

Original Article

Tumor treating fields induced senescence on glioblastoma

Eun Ho Kim

Department of Biochemistry, School of Medicine, Daegu Catholic University, 33, 17-gil, Duryugongwon-ro, Namgu, Daegu 42472, Korea

Received March 30, 2023; Accepted November 6, 2023; Epub November 15, 2023; Published November 30, 2023

Abstract: Innovative approaches have given rise to a method for treating newly diagnosed GBM cancer patients within a span of 4.9 months, resulting in improved median overall survival (OS) and minimal side effects during the phase III clinical trial. This approach is referred to as Tumor Treating Fields (TTFields). The objective of this study is to ascertain the potential of TTFields treatment in sensitizing GBM cancer cells by enhancing TTFields-induced senescence. To achieve this, the research employed a multifaceted methodology that encompassed several elements, including the analysis of SA-β-gal staining, flow cytometry, Western blotting, morphology assessment, Positron Emission Tomography (PET)/Computed Tomography (CT), immunohistochemical staining, and microassay. Over a period of up to 5 days, the number of cells exhibiting senescence-specific morphology and positive SA-β-Gal activity progressively increased. These findings indicate that p16, p21, p27 and pRB are pivotal regulators of TTFields-induced senescence through NF-κB activation. The outcomes reveal that TTFields treatment effectively promotes TTFields-induced senescence in GBM cells through a mechanism independent of apoptosis. In conclusion, this research underscores the viability of this treatment approach as a reliable protocol to address the limitations associated with the conventional GBM treatment.

Keywords: Tumor-treating fields, senescence, glioblastoma

Introduction

In a clinical phase III trial, the application of tumor treating fields (TTFields) at a frequency of 200 kHz, which is a newly approved method for treating GBM, resulted in an extended median overall survival (OS) of 4.9 months among primary GBM patients. Remarkably, this treatment exhibited mild side effects and did not lead to a deterioration in the patients' quality of life [1-3]. These alternating electric fields span a frequency range from 100 to 300 kHz with an amplitude of 1-3 V/cm [4, 5]. Ceramic electrodes, often referred to as transducer arrays, are affixed to the patient's shaved scalp for the precise delivery of these fields at tumor-specific frequencies during clinical applications. It was noted that treatment compliance had a significant impact on outcomes, with higher overall survival linked to monthly compliance rates exceeding 75% [6, 7]. This breakthrough in GBM patient treatment may potentially open doors to the incorporation of synergistic therapies to further enhance its efficacy [8, 9].

Our investigation focused on understanding the mechanism of action of TTFields in the search for novel facilitating agents. TTFields were found to inhibit the formation of spindles and affect other dipole macromolecules crucial for cell division, such as septins. This interference may lead to mitotic catastrophe, ultimately resulting in cell death [10, 11]. Additional impacted biological processes encompass apoptosis, autophagy, DNA repair, and immunogenic cell death [10, 12]. However, limited knowledge is available regarding the molecular biological processes underpinning TTFields-based cancer therapy.

Intrinsic and extrinsic stress, such as ionizing radiation (IR), can induce cellular senescence, characterized by an irreversible halt in the cell cycle [13-15]. Senescence diminishes a cell's lifespan and proliferative capacity, making it a key mechanism for cancer prevention [16, 17]. The main drivers of senescence include telomere shortening, DNA damage, oncogene activation, tumor suppressor inactivation, tumor

suppressor reactivation, and various other factors [18-22]. The p53 and p16-pRb pathways are primarily responsible for governing senescence [21]. The DNA damage response (DDR) activates p53, leading to senescence-related growth arrest by promoting the production of p21, a cyclin-dependent kinase (CDK) inhibitor [23]. It has also been suggested that various anti-cancer drugs, including IR, impede tumor cell growth through therapy-induced senescence [24]. Recent research has shown that radiation therapy-induced cell death in lung cancer cells is predominantly attributed to the induction of senescence rather than apoptosis, suggesting that the promotion of premature senescence may be crucial in mediating the anti-cancer effects of radiation therapy. Given the biological similarities between TTFields and radiotherapy mechanisms [8], we hypothesized that TTFields could also induce senescence [25]. TTFields exhibit anti-tumor effects by inhibiting growth, invasion, migration, or by triggering apoptosis or autophagic cell death [8, 26, 27]. Consequently, this study aimed to investigate whether TTFields treatment could enhance TTFields-induced senescence, along with IR, and to elucidate how TTFields treatment accelerates cell death in GBM cells via an apoptosis-independent mechanism.

Materials and methods

Cell culture and tissue samples

Human glioblastoma U87 and U373 cells were procured from the Korean Cell Line Bank located in Seoul, South Korea. U87 cells were cultured in MEM (Minimum Essential Medium) with the addition of 10% fetal bovine serum (FBS), glutamine, HEPES, and antibiotics. These cultures were maintained at 37°C in a humidified incubator under 5% CO_2. In parallel, U373 cells were cultivated in RPMI 1640 medium supplemented with 10% FBS, glutamine, HEPES, and antibiotics under similar incubation conditions. Patient-derived GBM stem cells, specifically the 528NS variant, were sourced from Dr. Ichiro Nakano at the University of Alabama at Birmingham, Birmingham, AL [28]. GSC 528 spheres (528NS) were nurtured in a defined medium comprising Dulbecco's modified Eagle's medium (DMEM)/F12 enriched with 0.1% B27, 0.1% gentamicin, 20 ng/mL basic fibroblast growth factor, and 20 ng/mL epidermal growth factor (Invitrogen). To induce differentiation in 528NS cells, they were exposed to the defined medium consisting of DMEM/F12 supplemented with 10% fetal bovine serum, 0.1% B27, and 0.1% gentamicin for a duration of 12 days [29-31].

Experimental setup of electric fields

A pair of insulated cables connected to an operational generator and a high-voltage amplifier were utilized for the generation of TTFields, as documented in a prior study [32]. This setup emitted sine-wave transmissions spanning from 0 V to 800 V, thereby producing an applied electric field characterized by a strength and frequency of 0.9 V/cm and 150 kHz. Given its widespread application in clinical contexts, a field intensity of 1.0 V/cm was selected for the purposes of this study. Cells were cultivated between 100-mm plates and maintained at a temperature of 37°C in a humid environment with 5% atmospheric CO_2 until they reached a confluence of 70-80% for subsequent irradiation treatment.

Reagents

Antibodies targeting p16, p21, p27, pRB, p-p65, and p-Ikb alpha were acquired from Cell Signaling Technology in Danvers, MA, USA. Additionally, antibodies against beta-actin, p16, p21, and p27 were procured from Santa Cruz Biotechnology in Dallas, TX, USA.

SA-β-gal staining

The assessment of cellular SA-β-gal activity was conducted following a previously outlined protocol [33]. Cells were cultivated to a density of 2×10^4 cells in 35-mm culture dishes, then subjected to PBS washing and fixation with 3.7% paraformaldehyde (v/v) at room temperature for a duration of 10 minutes. Subsequently, the cells were exposed to a staining solution that consisted of 1 mg/ml 5-bromo-4-chloro-3-indolyl-β-D-galactoside, 40 mM citric acid-sodium phosphate (pH 6.0), 5 mM potassium ferricyanide, 5 mM potassium ferrocyanide, 150 mM NaCl, and 2 mM $MgCl_2$ for a period of 16 hours at 37°C. Following this staining process, the SA-β-gal stained cells underwent PBS washing, followed by counterstaining with a 1% eosin solution for 5 minutes. Subsequently, the cells were washed twice with

ethanol. The percentage of blue-stained cells was calculated, with the count being based on every 400 cells observed under a light microscope.

MTT assay

For the quantification of cell viability, an equivalent volume of culture medium containing the EZ-Cytox reagent (EZ3000, Daeillab Service, Chungcheongbuk-do, Republic of Korea) was introduced to the cells, and this mixture was allowed to incubate for a period of 4 hours. Subsequently, cell viability was assessed by measuring the absorbance at 450 nm using a Multiskan EX spectrophotometer (Thermo Fisher Scientific; Waltham, MA, USA).

Western blotting

The GBM cells were treated with TTFields and subsequently incubated for a duration of 5 days. Following the incubation, cell lysis was carried out using RIPA buffer, and the proteins were then separated through sodium-polyacrylamide gel electrophoresis before being transferred onto nitrocellulose membranes. These membranes were subsequently subjected to blocking with a 1% (v/v) solution of non-fat dried milk in Tris-buffered saline with 0.05% Tween-20. Further steps involved the incubation of the membranes with the necessary antibodies. Primary antibodies were employed at a dilution of 1:1,000, while secondary antibodies were used at a dilution of 1:5,000. Immunoreactive protein bands were visualized through enhanced chemiluminescence (Amersham Biosciences) and then scanned. The ImageJ program was utilized to calculate the rate of change in the expression level of the target protein in comparison to the control.

Morphology

To investigate the impact of TTFields on cell morphology, cells subjected to TTFields treatment were stained using Giemsa. In a nutshell, cells that were initially seeded in six-well plates were permitted to adhere to cover slips overnight before undergoing TTFields treatment. Subsequently, the cells were fixed with methanol for a duration of 10 minutes and then stained with Giemsa (at a concentration of 10% in PBS) for 15 minutes, followed by a thorough washing with tap water. Images were captured using a Nikon Eclipse Ts2R-FL microscope.

Tumor xenografts in nude mice

Subcutaneous injections of 528NS GBM patient stem cells (1×10^6 cells) were administered into the hindquarters of 5-week-old BALB/c nude mice sourced from Nara Biotech in Gyeonggi-do, Republic of Korea. Once the tumor had reached a minimal volume falling within the range of 100-200 mm^3, the mice were randomly divided into two groups, each consisting of 5 mice. The allocation of mice to their groups was conducted in a blinded manner. The grouping was based on average tumor volume. Subsequently, TTFields at an intensity of 1 V/cm were initiated and maintained for a duration of 7 days. The tumor volume was calculated using the formula $(L \times l^2)/2$, where measurements of tumor length (L) and breadth (l) were obtained with a caliper. It's worth noting that this trial received approval from the Korea University Institutional Review Board (KUIACUC-2018), and all relevant international and institutional guidelines governing the care and utilization of animals were adhered to.

Acquisition technique of positron emission tomography (PET)/computed tomography (CT)

PET images were acquired using a Siemens Inveon PET scanner from Siemens Medical Solutions in Erlangen, Germany. To prepare the mice, they were gently warmed using a heating pad before being given ^{18}F-fluoro-2-deoxy-d-glucose ([^{18}F]-FDG) orally. They were then injected with 200 μCi of [^{18}F]-FDG through their tail veins while under anesthesia, which was administered as a solution of 200 μCi of [^{18}F]-FDG (Forane solution, ChoongWae Pharma, Seoul, Korea). The acquisition of anatomical images was made possible by collecting X-Ray CT data of the mice using the Inveon system, involving an 80-degree projection and full rotation. The X-ray CT exposure lasted for 200 milliseconds, with a predicted scan time of 504 seconds. The reconstruction of the X-ray CT data was carried out using the Feldkamp method, which utilizes Shepp and Logan filters [L.A. Feldkamp et al., Dearborn, MI, USA]. The resulting X-ray CT images had a pixel size of 109.69 μm × 109.69 μm. After 30 minutes of tracer uptake and X-ray CT data collection, PET data was acquired over a 15-minute duration within the energy range of 350-650 keV. Emission list-mode PET data was collected to generate 3D sinograms, and their reconstruction was per-

formed using OSEM2D techniques. The reconstructed images had a pixel size of 0.38 × 0.38 × 0.79 mm^3.

Various necessary corrections, including normalization, random rectification, and dead-time correction, were applied to all datasets. Regions of Interest (ROIs) were defined using X-ray CT data. The coregistration of CT and PET images was facilitated by Inveon Research Workplace (version 2.0, Erlangen, Germany) from Siemens Medical Solutions. Using a predetermined conversion criterion, the highest pixel values within the ROIs on the PET image were assessed and converted to radioactive counts per minute (cpm) values.

Immunohistochemical staining (IHC)

For the purpose of immunohistochemical evaluations, 4-μm-thick sections of paraffin-embedded tissue were affixed to glass slides coated for the detection of the target proteins. After antigen retrieval and the inhibition of endogenous peroxidases and non-specific protein binding, the slide sections were subjected to an initial incubation with primary antibodies. Subsequently, appropriate horseradish peroxidase-conjugated secondary antibodies were applied. To visualize the results, all slides were developed using 3,3'-diaminobenzidine and were subsequently counterstained with hematoxylin.

Microarray analysis

Total RNA was extracted from both induced control and TTFields-treated cells using TRIzol (Invitrogen, Carlsbad, CA, USA). Subsequently, the extracted RNA was purified utilizing the RNeasy Mini Kit from Qiagen in Hilden, Germany, following the manufacturer's provided guidelines. The quality of the RNA was evaluated using an Agilent 2100 Bioanalyzer (Agilent, Palo Alto, CA, USA). Only high-quality RNA samples, characterized by a RNA integrity number exceeding 9.0, were utilized for the gene expression microarray analysis.

In the microarray analysis, 100 ng of total RNA was processed to generate biotin-labeled targets, which were then subjected to hybridization with the Affymetrix Gene 1.0 ST array, following the manufacturer's protocols. This approach was adopted to conduct gene expression profiling experiments, with Affymetrix, Inc. in Santa Clara, CA, USA, providing the necessary materials and support.

RNA isolation and cDNA synthesis

To extract the cells, they were subjected to trypsinization and then suspended in TRIzol from Invitrogen, based in Carlsbad, CA, USA. The subsequent isolation of total RNA was carried out using the RNeasy Mini Kit provided by Qiagen, located in Hilden, Germany, following the manufacturer's recommended procedures. For the synthesis of cDNA, the QuantiTect Reverse Transcription Kit, also from Qiagen, was employed. To initiate this process, 1 μg of total RNA was combined with 2 μl of gDNA Wipeout Buffer, and then DEPC water was added to reach a total volume of 14 μl. This mixture was incubated at 42°C for 2 minutes. Subsequently, the blend was mixed with Quantiscript RT Buffer, RT Primer Mix, and Quantiscript Reverse Transcriptase, and incubated at 42°C for 45 minutes. The reaction was then subjected to an incubation at 95°C for 2 minutes and allowed to cool down to room temperature.

Statistical analysis

Statistical significance was assessed using an ANOVA statistical test, and the analysis was conducted with Prism 6 software, located in La Jolla, California, USA. In the text, the degree of statistical significance is indicated based on the associated *P* values. Specifically, the following conventions were used: *, denoting $P < 0.05$; **, denoting $P < 0.01$; and ***, denoting $P < 0.001$, to indicate statistically significant results.

Results

TTFields restrict the development of GBM tumor xenograft implants in mice

The TTFields was aimed using insulated wires connected to a generator and an amplifier to generate a sine-wave signal ranging between 0-800 V (**Figure 1A**). To investigate the potential of TTFields in inhibiting GBM growth in vivo, we transplanted surgically excised tumors derived from 528NS GBM patient stem cells into Balb/C mice. Following TTFields treatment, we observed a reduction in the number of Ki67-

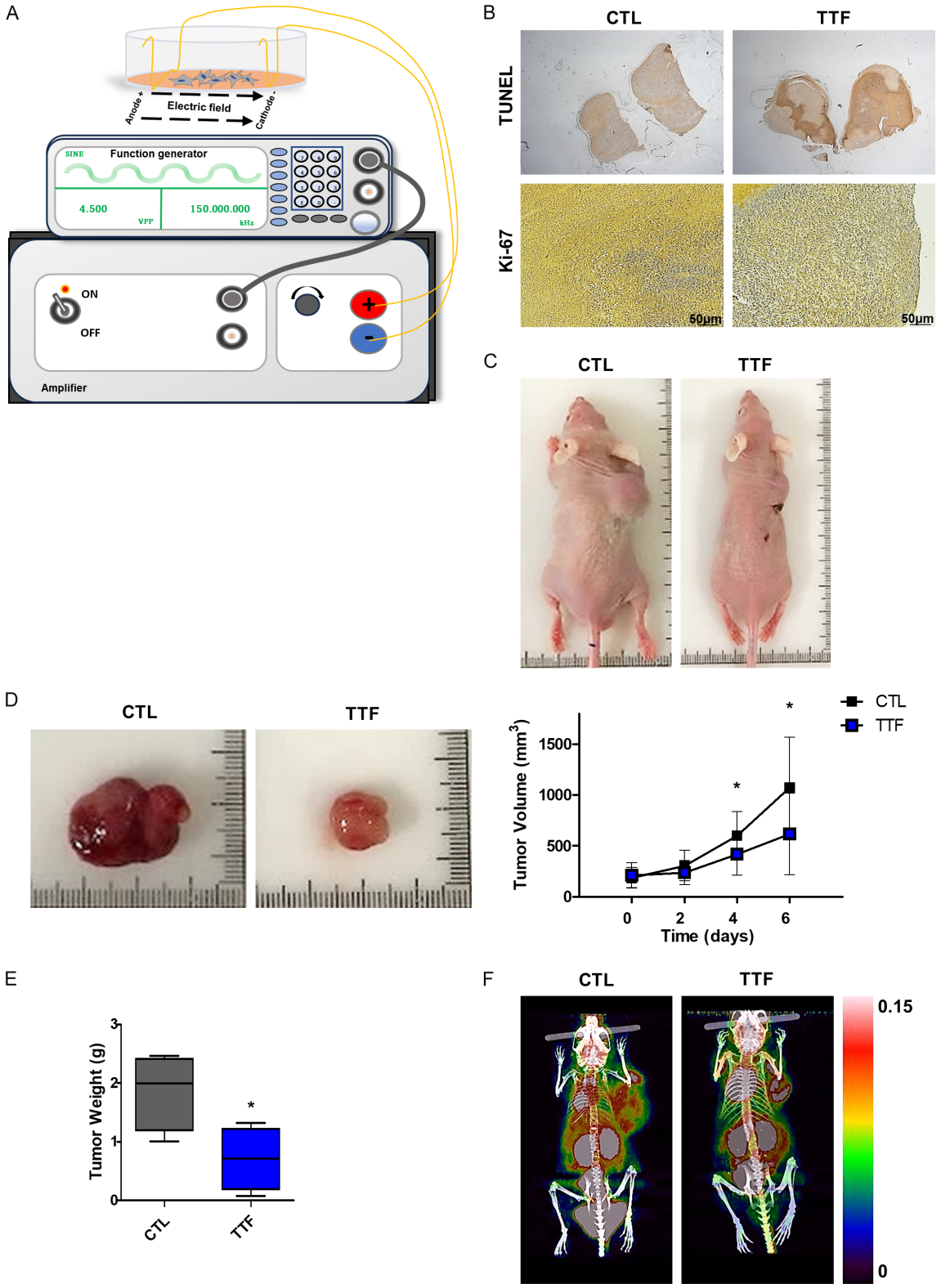

Figure 1. TTFields-sensitizing effect in *in vivo* models using GBM patient stem cells. A. Schematic of the experimental setup for TTFields treatment. B. TUNEL assay and immunohistochemistry for Ki-67 expression were performed using xenografts. C. Representative images of 528NS GBM patient cells tumor-bearing mice after injection. D. Nude mice were injected with 528NS cells lines and then treated with TTFields. Tumor volumes were measured by: volume = (length × width^2 × 3.14)/6 (n = 5). Tumors were excised and weighed at the end of the experiment (7 days). E. The tumor weights of the mice with TTFields therapy-treated groups. F. PET/CT imaging of 528NS tumor-bearing mice after fluorine-18-fluorodeoxyglucose ([^{18}F]-FDG) injection and subsequent anesthesia. The [^{18}F]-FDG radioactivity is presented as the maximal standardized uptake value (mean ± standard deviation).

positive cells and an increase in the quantity of TUNEL-positive cells within the xenograft tumor tissue. Ki67 and TUNEL are established biomarkers for proliferation and apoptosis, respectively (as depicted in **Figure 1B**). Tumors treated with TTFields exhibited a notably slower rate of growth compared to the control group (as shown in **Figure 1C**). Furthermore, at the macroscopic level, the TTFields-treated tumors were significantly smaller than those in the control group (illustrated in **Figure 1D**). On average, mice subjected to TTFields treatment had notably smaller tumor volumes than those in the control group (illustrated in **Figure 1E**). Additionally, GBM tumors treated with TTFields displayed reduced absorption of [^{18}F]-FDG compared to the control groups, as shown in **Figure 1F**. Notably, when TTFields were directed towards the tumors, there was a remarkable 70% reduction in tumor volume in TTFields-treated mice compared to those treated with the control vehicle (as presented in **Figure 1C**). These findings provide compelling evidence that TTFields have a substantial inhibitory effect on tumor growth.

TTFields result in senescence in vitro

In spite of previous research highlighting the extensive induction of apoptosis by TTFields in various human cancers [4, 8, 34, 35], our investigation revealed a distinct pattern of cell cycle arrest and apoptosis in tumor implants from GBM patients treated with TTFields. Through in vitro experiments, we observed that TTFields treatment led to a significant reduction in the number of viable cells, as depicted in **Figure 2A**. Although TTFields did induce some level of apoptosis in GBM cell lines, it was insufficient to explain the substantial decrease in cell numbers observed across all three GBM cell lines tested, as shown in **Figure 2B**. This discrepancy led us to hypothesize that other mechanisms were at play in suppressing tumor growth in response to TTFields, particularly because the degree of apoptosis alone could not account for the marked reduction in cell numbers. One distinctive change we noted was a significant increase in cellular size after five days of TTFields treatment in vitro, as presented in **Figure 2C**, a characteristic indicative of senescence. To verify if this observed phenotype was indeed due to senescence, we conducted β-galactosidase activity analysis (SA-β-Gal staining), and the results confirmed significant senescence in the stem cells xenograft tumor obtained from the GBM patient who had received TTFields treatment. For further validation, we compared morphological alterations in GBM cells treated with ionizing radiation (IR), as the process through which IR induces senescence is well-established [36, 37]. The exposure to IR significantly reduced the cells' proliferative capacity while progressively inducing morphological changes associated with senescence, such as an enlarged and flattened cellular shape. This observed morphological transformation aligned with the senescence phenotype reported in IR-treated cells [36, 38].

To ascertain the influence of TTFields on senescence induction, we monitored cellular morphology and SA-β-Gal activity over a span of five days. Over this duration, an increasing number of cells displayed senescence-specific morphology and exhibited positive SA-β-Gal activity, as illustrated in **Figure 2D**. The induction of senescence also led to a substantial reduction in cell growth, with nearly all cells staining positively for SA-β-Gal after five days.

TTFields activate the p16-p21-p27 signaling pathway in GBM cells

Regarding the molecular mechanism behind TTFields-induced cell senescence, the p53-p21-RB pathway and the p16-RB pathway are pivotal molecular pathways responsible for inducing cell cycle arrest [39-42]. To determine the expression of p16, p21, p27, and RB in GBM cells exposed to TTFields for five days, we conducted PCR analysis and western blot analysis. The results indicated that TTFields significantly up regulated the expression of p16, p21, and p27 in GBM cells, as illustrated in **Figure 3A**. The increased expression of p16, p21, and p27 in GBM cells after five days of TTFields treatment was further validated through western blot analysis, consistent with the findings from PCR analysis, as demonstrated in **Figure 3B**.

Of particular note, tumor implants generated from patient stem cells obtained from 528NS GBM exhibited significantly higher expression levels of p16, p21, and p27 and lower levels of pRB after being treated with TTFields, as determined through immunohistochemical (IHC) analysis, as depicted in **Figure**

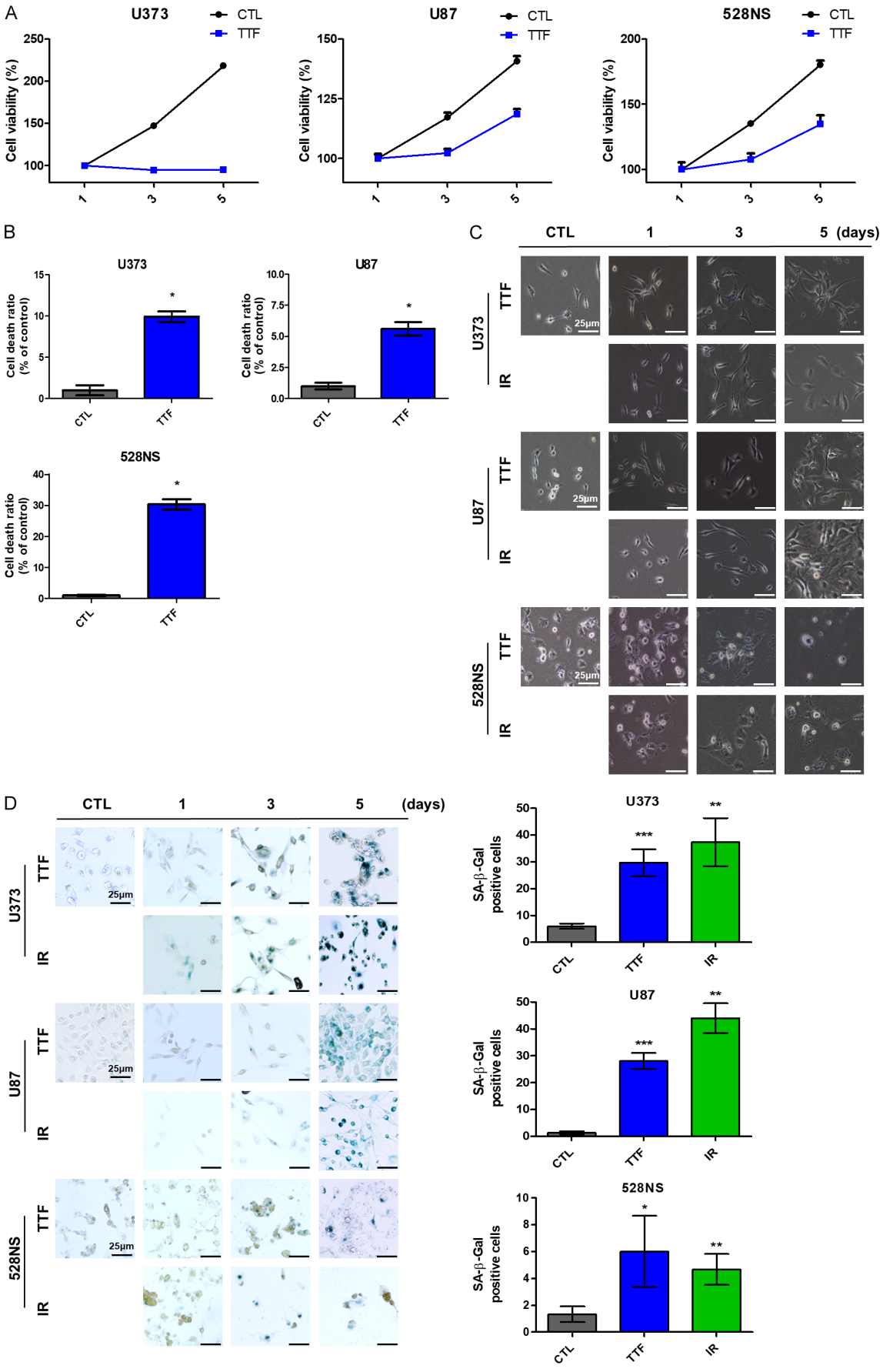
A
U373
U87
528NS
CTL
TTF
Cell viability (%)
B
Cell death ratio (% of control)
C
CTL
1
3
5 (days)
TTF
IR
25μm
D
SA-β-Gal positive cells

Figure 2. Changes in cell morphology and senescence-associated β-galactosidase activity in GBM cells following exposure to TTFields. A. The proliferation rate was detected by MTT assay. B. U373 and U87 cells were exposed to TTFields for 5 days prior to annexin V/PI staining. C. U87, U373 and 528NS stem cells exposed to TTFields presented an enlarged cellular volume and altered shape, resembling the typical senescent phenotype. D. The percentage of SA-β-gal-positive stained cells increased to 3 times when exposed to TTFields, respectively, compared with the control cells.

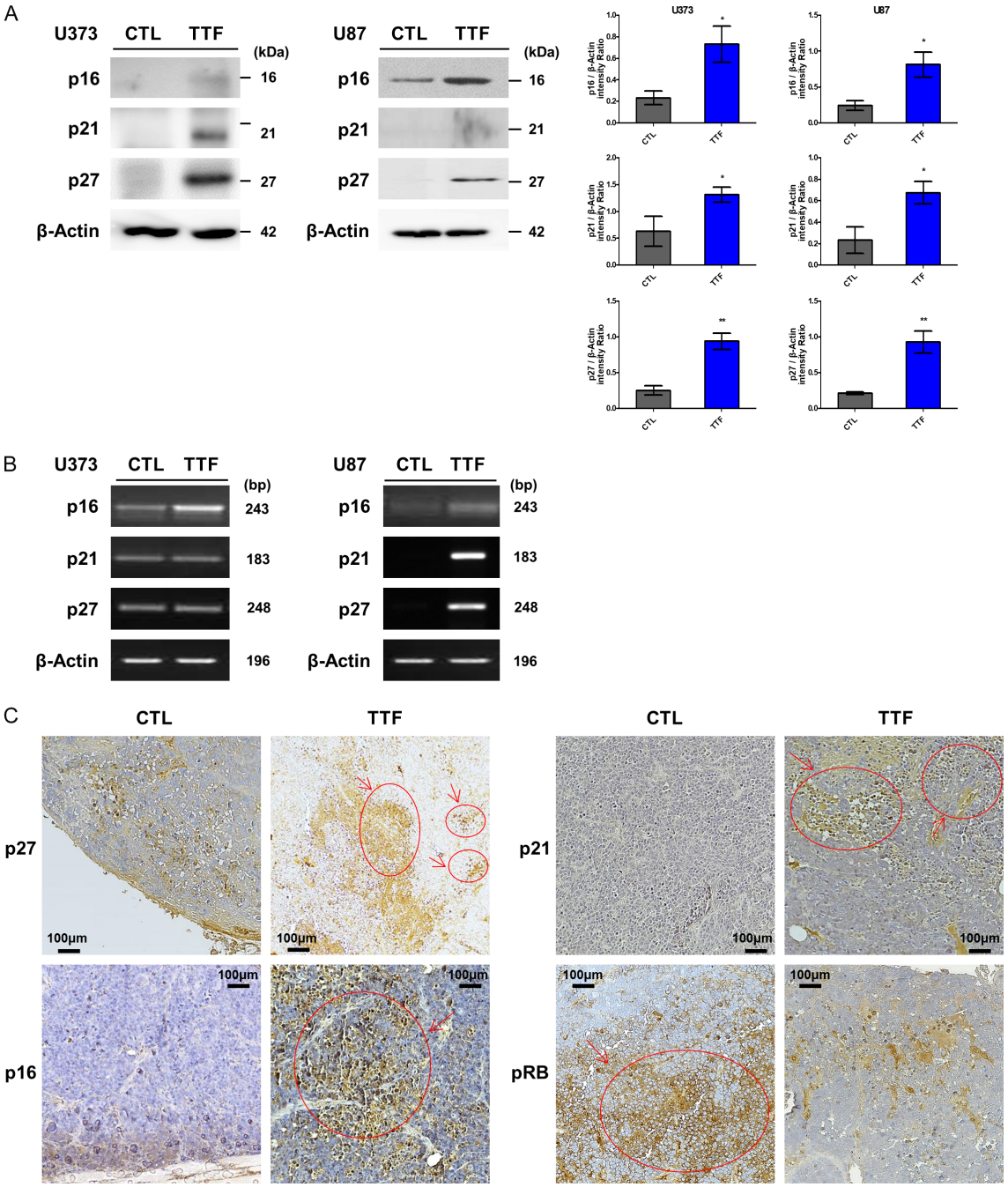

Figure 3. The activation of the p16-p21-retinoblastoma protein (Rb) pathway induced by TTFields. A and B. The quantitative PCR analysis and western blot analysis of p16, p21 and p27 in 2 GBM cells subjected to TTFields for 5 days. C. Immunohistochemistry for p27, p16, p21 and pRb expression level in the xenografts.

3C. These findings collectively indicate that p16, p21, and p27 act as critical regulators of TTFields-induced senescence. Taken together, the analyses confirm that TTFields treatment is indeed capable of triggering senescence.

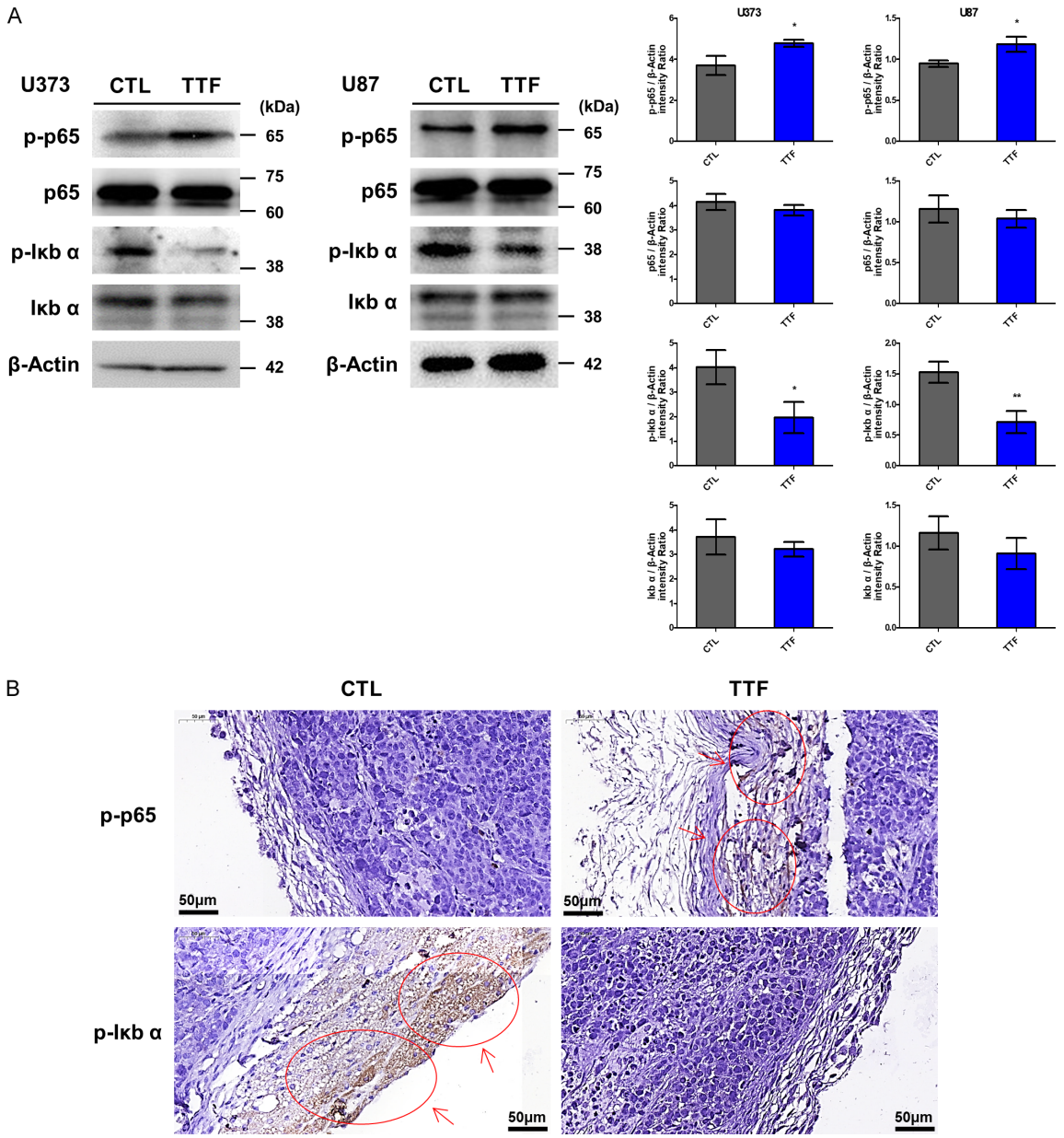

Figure 4. Validation of the NF-Kb after TTFields treatment. A. Western blotting for p-p65, p65, p-IκB-α and IκB-α expression in 2 GBM cells. B. Immunohistochemistry for p-p65 and p-IκB-α expression level in the 528NS patient stem cell xenografts.

Therapy-induced senescence initiates the senescence via NF-κB activation

Cellular senescence and apoptosis represent two pivotal physiological and biochemical processes that involve the NF-κB signaling pathway [43, 44, 45]. To determine whether NF-κB induction plays a role in modulating cellular senescence following TTFields treatment, we conducted Western blot and IHC analyses to assess the levels of phosphorylated NF-κB p65 (p-p65 S536) and IκB-α. The results demonstrated that TTFields treatment led to an increase in p-p65 levels and a decrease in its inhibitory regulator, IκB-α, as depicted in **Figure 4A** and **4B**.

These findings suggest that TTFields treatment induces NF-κB signaling, which may contribute to the modulation of cellular senescence.

Expression of marker genes showing senescence according to time after TTFields

Microarray analysis was employed on both control and TTFields-treated cells to investigate potential senescence-associated pathways. The results indicated a significant association, represented by a Pearson correlation coefficient $|r| > 0.9$, and a substantial change (ANOVA *p*-value within 1 per cent FDR) over time, which allowed us to identify marker genes that represent senescence-related characteristics (**Figure 5A**). This analysis revealed that 3 to 18% of genes displayed a positive correlation, indicating a gradual up-regulation, while 4 to 10% of genes showed a negative correlation, indicating a gradual down-regulation after exposure to TTFields. Furthermore, gene expression profiling revealed that several senescence-related genes exhibited a ≥ 2-fold increase in expression after 5 days of treatment (**Figure 5B**), providing additional confirmation of the role of senescence in TTFields-induced cell death. These genes may serve as conventional senescence indicators for TTFields treatment, and the functional assessments strongly suggest that alterations in their expression may underlie the observed senescence phenotypes following TTFields exposure.

Discussion

Despite TTFields therapy's current application in clinical settings, the precise mechanism by which it regulates cancer cells remains an enigma. Recent research has unveiled a novel aspect of TTFields therapy, revealing that it induces senescence and apoptosis in GBM cells. The presence of TTFields inhibits cell proliferation and elevates the number of senescent cells marked by SA-β-gal, indicating that the delay in cancer cell growth due to TTFields encourages cellular senescence.

The induction of senescence is a significant alternative mechanism for tumor suppression, well-documented in the context of chemotherapy and radiotherapy [24, 25, 46]. This study has unveiled a groundbreaking finding that TTFields sensitize cancer cells to senescence alongside apoptosis, in contrast to the prevailing focus on inducing tumor cell apoptosis in previous TTFields research [8, 35, 47, 48]. In the current TTFields therapy regimen, which combines radiation and chemotherapy for cancer treatment, senescence can be achieved with notably lower chemotherapeutic doses compared to apoptosis. This bears importance as senescence is associated with better therapeutic responses in cancer cases. Therefore, this TTFields strategy holds promise in mitigating the adverse effects of cancer therapy, particularly in the context of combined chemo or radiotherapy, thereby enhancing the quality of life and life expectancy for cancer patients in clinical practice.

Prior studies have suggested that TTFields may inhibit GBM growth by inducing tumor cell apoptosis, mediated by elevated Caspase-3 and decreased Bcl-x [8]. This study further underscores the significance of cell senescence, which involves the up regulation of various genes, including p16, p21, and p53 [49]. The research findings substantiate the notion that TTFields promote senescence in GBM cells, as evidenced by SA-β-gal staining and Western blot results, demonstrating increased expression levels of p16, p21, and p53.

Moreover, TTFields treatment is found to boost the expression of p53 and p21, which are pivotal for triggering senescence. This aligns with the activation of p53-dependent senescence by various medications such as adenosine and metformin [50, 51]. Inducing a growth-inhibitory response is considered an innovative approach, as anticancer treatment has previously been observed to induce a senescent state in cancer cells, especially relevant in clinical settings [52]. The creation of a senescence response has proven effective in treatment strategies that either activate p21 or reactivate p53 [53, 54].

This study primarily concentrates on senescence in human GBM, owing to its potential to revolutionize cancer treatment and inspire novel therapies. The research definitively demonstrates that TTFields-induced tumor senescence impedes GBM tumor growth in mice. Nevertheless, the study has limitations, such as not investigating senescence control in normal cell lines and the uncharted territory of long-term implications of senescence on tumor growth. Additional research is warranted to discern whether TTFields exert a similar impact on other cancer types.

In summary, TTFields therapy presents a promising avenue to transcend the limitations of conventional GBM treatment. It effectively miti-

A

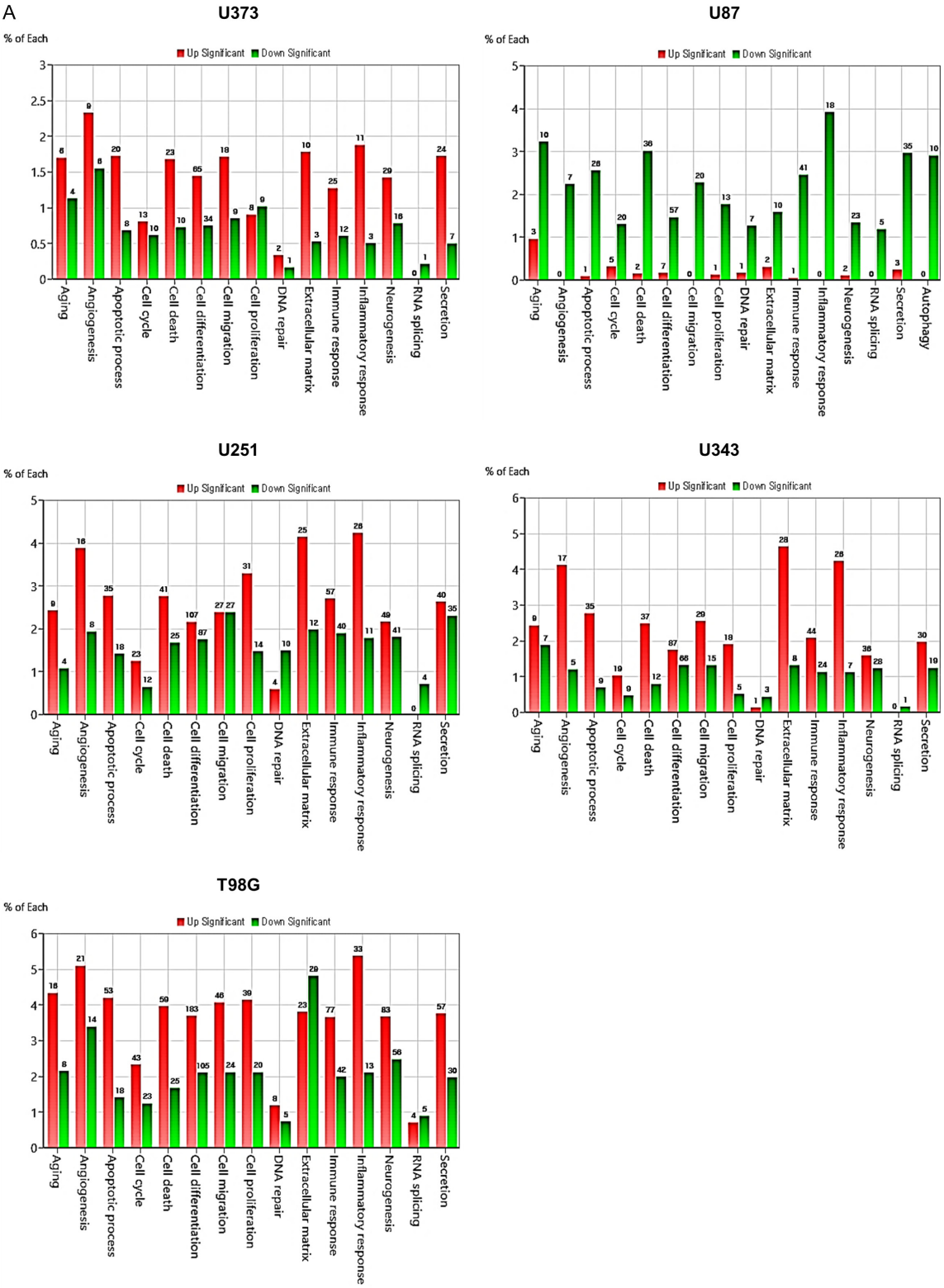
U373
% of Each
Up Significant
Down Significant
Aging
Angiogenesis
Apoptotic process
Cell cycle
Cell death
Cell differentiation
Cell migration
Cell proliferation
DNA repair
Extracellular matrix
Immune response
Inflammatory response
Neurogenesis
RNA splicing
Secretion
U87
% of Each
Up Significant
Down Significant
Aging
Angiogenesis
Apoptotic process
Cell cycle
Cell death
Cell differentiation
Cell migration
Cell proliferation
DNA repair
Extracellular matrix
Immune response
Inflammatory response
Neurogenesis
RNA splicing
Secretion
Autophagy
U251
% of Each
Up Significant
Down Significant
Aging
Angiogenesis
Apoptotic process
Cell cycle
Cell death
Cell differentiation
Cell migration
Cell proliferation
DNA repair
Extracellular matrix
Immune response
Inflammatory response
Neurogenesis
RNA splicing
Secretion
U343
% of Each
Up Significant
Down Significant
Aging
Angiogenesis
Apoptotic process
Cell cycle
Cell death
Cell differentiation
Cell migration
Cell proliferation
DNA repair
Extracellular matrix
Immune response
Inflammatory response
Neurogenesis
RNA splicing
Secretion
T98G
% of Each
Up Significant
Down Significant
Aging
Angiogenesis
Apoptotic process
Cell cycle
Cell death
Cell differentiation
Cell migration
Cell proliferation
DNA repair
Extracellular matrix
Immune response
Inflammatory response
Neurogenesis
RNA splicing
Secretion

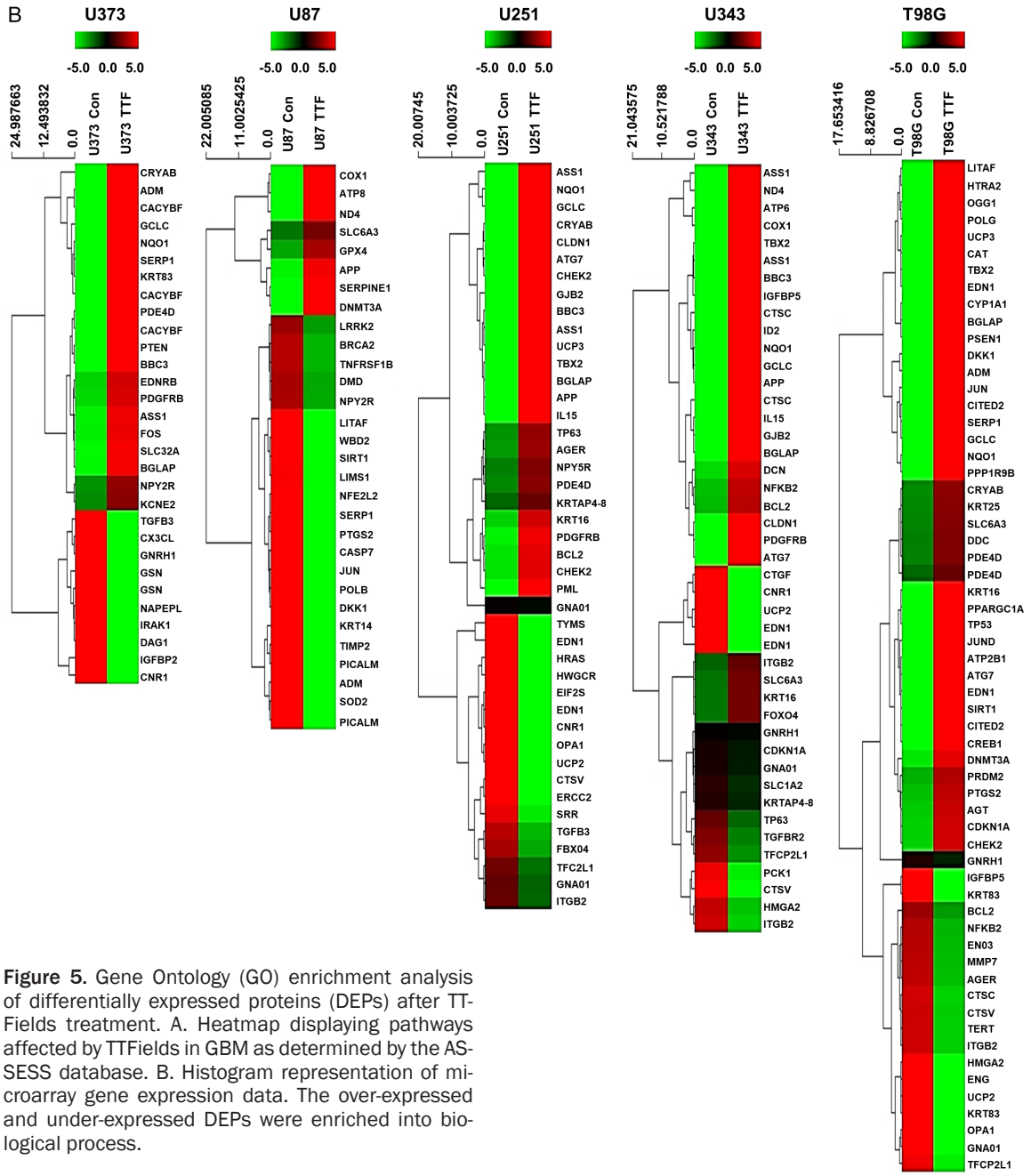

Figure 5. Gene Ontology (GO) enrichment analysis of differentially expressed proteins (DEPs) after TTFields treatment. A. Heatmap displaying pathways affected by TTFields in GBM as determined by the ASSESS database. B. Histogram representation of microarray gene expression data. The over-expressed and under-expressed DEPs were enriched into biological process.

gates the malignancy of GBM cells by preferentially inducing senescence. Although further research is required to integrate TTFields into GBM patients' treatment regimens, the study underscores the importance of TTFields in GBM treatment. It introduces the concept that senescence induction in cancer cells is a pivotal biological mechanism of TTFields, in addition to the well-known mechanisms encompassing apoptosis, DNA damage, and autophagy. These findings not only provide invaluable insights into TTFields' anticancer mechanisms but also shed light on a novel approach for regulating senescence in GBM, offering new prospects for cancer treatment.

Acknowledgements

This work was supported by the research grants from Daegu Catholic University in 2023.

Disclosure of conflict of interest

None.

Address correspondence to: Dr. Eun Ho Kim, Department of Biochemistry, School of Medicine, Daegu Catholic University, 33, 17-gil, Duryugongwon-ro, Nam-gu, Daegu 42472, Korea. Tel: 8253650-4480; E-mail: eh140149@cu.ac.kr

References

[1] Stupp R, Taillibert S, Kanner A, Read W, Steinberg D, Lhermitte B, Toms S, Idbaih A, Ahluwalia MS, Fink K, Di Meco F, Lieberman F, Zhu JJ, Stragliotto G, Tran D, Brem S, Hottinger A, Kirson ED, Lavy-Shahaf G, Weinberg U, Kim CY, Paek SH, Nicholas G, Bruna J, Hirte H, Weller M, Palti Y, Hegi ME and Ram Z. Effect of tumor-treating fields plus maintenance temozolomide vs maintenance temozolomide alone on survival in patients with glioblastoma: a randomized clinical trial. JAMA 2017; 318: 2306-2316.

[2] Zhu JJ, Demireva P, Kanner AA, Pannullo S, Mehdorn M, Avgeropoulos N, Salmaggi A, Silvani A, Goldlust S, David C and Benouaich-Amiel A; Zvi Ram on behalf of the EF-14 Trial Investigators. Health-related quality of life, cognitive screening, and functional status in a randomized phase III trial (EF-14) of tumor treating fields with temozolomide compared to temozolomide alone in newly diagnosed glioblastoma. J Neurooncol 2017; 135: 545-552.

[3] Teoh E, Bottomley D, Scarsbrook A, Payne H, Afaq A, Bomanji J, Van As N, Chua S, Hoskin P, Chambers A, Cook GJ, Warbey VS, Chau A, Ward P, Miller MP, Stevens DJ, Wilson L and Gleeson FV. Impact of 18F-fluciclovine PET/CT on clinical management of patients with recurrent prostate cancer: results from the phase 3 FALCON trial. Int J Radiat Oncol Biol Phys 2017; 99: 1316-1317.

[4] Kirson ED, Gurvich Z, Schneiderman R, Dekel E, Itzhaki A, Wasserman Y, Schatzberger R and Palti Y. Disruption of cancer cell replication by alternating electric fields. Cancer Res 2004; 64: 3288-3295.

[5] Davies AM, Weinberg U and Palti Y. Tumor treating fields: a new frontier in cancer therapy. Ann N Y Acad Sci 2013; 1291: 86-95.

[6] Kanner AA, Wong ET, Villano JL and Ram Z; EF-11 Investigators. Post Hoc analyses of intention-to-treat population in phase III comparison of NovoTTF-100A™ system versus best physician's choice chemotherapy. Semin Oncol 2014; 41 Suppl 6: S25-34.

[7] Mrugala MM, Engelhard HH, Dinh Tran D, Kew Y, Cavaliere R, Villano JL, Annenelie Bota D, Rudnick J, Love Sumrall A, Zhu JJ and Butowski N. Clinical practice experience with NovoTTF-100A™ system for glioblastoma: the patient registry dataset (PRiDe). Semin Oncol 2014; 41 Suppl 6: S4-S13.

[8] Kim EH, Kim YH, Song HS, Jeong YK, Lee JY, Sung J, Yoo SH and Yoon M. Biological effect of an alternating electric field on cell proliferation and synergistic antimitotic effect in combination with ionizing radiation. Oncotarget 2016; 7: 62267-62279.

[9] Kim JY, Jo Y, Oh HK and Kim EH. Sorafenib increases tumor treating fields-induced cell death in glioblastoma by inhibiting STAT3. Am J Cancer Res 2020; 10: 3475-3486.

[10] Kirson ED, Dbaly V, Tovarys F, Vymazal J, Soustiel JF, Itzhaki A, Mordechovich D, Steinberg-Shapira S, Gurvich Z, Schneiderman R, Wasserman Y, Salzberg M, Ryffel B, Goldsher D, Dekel E and Palti Y. Alternating electric fields arrest cell proliferation in animal tumor models and human brain tumors. Proc Natl Acad Sci U S A 2007; 104: 10152-10157.

[11] Giladi M, Schneiderman RS, Voloshin T, Porat Y, Munster M, Blat R, Sherbo S, Bomzon Z, Urman N, Itzhaki A, Cahal S, Shteingauz A, Chaudhry A, Kirson ED, Weinberg U and Palti Y. Mitotic spindle disruption by alternating electric fields leads to improper chromosome segregation and mitotic catastrophe in cancer cells. Sci Rep 2015; 5: 18046.

[12] Silginer M, Weller M, Stupp R and Roth P. Biological activity of tumor-treating fields in preclinical glioma models. Cell Death Dis 2017; 8: e2753.

[13] Wang Y, Scheiber MN, Neumann C, Calin GA and Zhou D. MicroRNA regulation of ionizing radiation-induced premature senescence. Int J Radiat Oncol Biol Phys 2011; 81: 839-848.

[14] Jones KR, Elmore LW, Jackson-Cook C, Demasters G, Povirk LF, Holt SE and Gewirtz DA. p53-dependent accelerated senescence induced by ionizing radiation in breast tumour cells. Int J Radiat Biol 2005; 81: 445-458.

[15] Schmitt CA. Cellular senescence and cancer treatment. Biochim Biophys Acta 2007; 1775: 5-20.

[16] Guo X, Keyes WM, Papazoglu C, Zuber J, Li W, Lowe SW, Vogel H and Mills AA. TAp63 induces senescence and suppresses tumorigenesis in vivo. Nat Cell Biol 2009; 11: 1451-1457.

[17] Braig M, Lee S, Loddenkemper C, Rudolph C, Peters AH, Schlegelberger B, Stein H, Dorken B, Jenuwein T and Schmitt CA. Oncogene-induced senescence as an initial barrier in lymphoma development. Nature 2005; 436: 660-665.

[18] Collado M and Serrano M. The power and the promise of oncogene-induced senescence markers. Nat Rev Cancer 2006; 6: 472-476.

[19] Lee M and Lee JS. Exploiting tumor cell senescence in anticancer therapy. BMB Rep 2014; 47: 51-59.

[20] Rodier F and Campisi J. Four faces of cellular senescence. J Cell Biol 2011; 192: 547-556.

[21] Campisi J and d'Adda di Fagagna F. Cellular senescence: when bad things happen to good cells. Nat Rev Mol Cell Biol 2007; 8: 729-740.
[22] Kuilman T, Michaloglou C, Mooi WJ and Peeper DS. The essence of senescence. Genes Dev 2010; 24: 2463-2479.
[23] Sabin RJ and Anderson RM. Cellular senescence - its role in cancer and the response to ionizing radiation. Genome Integr 2011; 2: 7.
[24] Ewald JA, Desotelle JA, Wilding G and Jarrard DF. Therapy-induced senescence in cancer. J Natl Cancer Inst 2010; 102: 1536-1546.
[25] Luo H, Yount C, Lang H, Yang A, Riemer EC, Lyons K, Vanek KN, Silvestri GA, Schulte BA and Wang GY. Activation of p53 with Nutlin-3a radiosensitizes lung cancer cells via enhancing radiation-induced premature senescence. Lung Cancer 2013; 81: 167-173.
[26] Kim EH, Song HS, Yoo SH and Yoon M. Tumor treating fields inhibit glioblastoma cell migration, invasion and angiogenesis. Oncotarget 2016; 7: 65125-65136.
[27] Kim EH, Jo Y, Sai S, Park MJ, Kim JY, Kim JS, Lee YJ, Cho JM, Kwak SY, Baek JH, Jeong YK, Song JY, Yoon M and Hwang SG. Tumor-treating fields induce autophagy by blocking the Akt2/miR29b axis in glioblastoma cells. Oncogene 2019; 38: 6630-6646.
[28] Yin J, Oh YT, Kim JY, Kim SS, Choi E, Kim TH, Hong JH, Chang N, Cho HJ, Sa JK, Kim JC, Kwon HJ, Park S, Lin W, Nakano I, Gwak HS, Yoo H, Lee SH, Lee J, Kim JH, Kim SY, Nam DH, Park MJ and Park JB. Transglutaminase 2 inhibition reverses mesenchymal transdifferentiation of glioma stem cells by regulating C/EBPbeta signaling. Cancer Res 2017; 77: 4973-4984.
[29] Joshi K, Banasavadi-Siddegowda Y, Mo X, Kim SH, Mao P, Kig C, Nardini D, Sobol RW, Chow LM, Kornblum HI, Waclaw R, Beullens M and Nakano I. MELK-dependent FOXM1 phosphorylation is essential for proliferation of glioma stem cells. Stem Cells 2013; 31: 1051-1063.
[30] Gu C, Banasavadi-Siddegowda YK, Joshi K, Nakamura Y, Kurt H, Gupta S and Nakano I. Tumor-specific activation of the C-JUN/MELK pathway regulates glioma stem cell growth in a p53-dependent manner. Stem Cells 2013; 31: 870-881.
[31] Mao P, Joshi K, Li J, Kim SH, Li P, Santana-Santos L, Luthra S, Chandran UR, Benos PV, Smith L, Wang M, Hu B, Cheng SY, Sobol RW and Nakano I. Mesenchymal glioma stem cells are maintained by activated glycolytic metabolism involving aldehyde dehydrogenase 1A3. Proc Natl Acad Sci U S A 2013; 110: 8644-8649.
[32] Oh JY, Lee YJ and Kim EH. Tumor-treating fields inhibit the metastatic potential of osteosarcoma cells. Technol Cancer Res Treat 2020; 19: 1533033820947481.
[33] Dimri GP, Lee X, Basile G, Acosta M, Scott G, Roskelley C, Medrano EE, Linskens M, Rubelj I, Pereira-Smith O, et al. A biomarker that identifies senescent human cells in culture and in aging skin in vivo. Proc Natl Acad Sci U S A 1995; 92: 9363-9367.
[34] Lee WS and Kim EH. Combination therapy of doxorubicin with TTFields and radiation: newer approaches to combat lung cancer. Am J Cancer Res 2022; 12: 2673-2685.
[35] Lee YJ, Cho JM, Sai S, Oh JY, Park JA, Oh SJ, Park M, Kwon J, Shin US, Beak JH, Lim SH, Song JY, Hwang SG and Kim EH. 5-fluorouracil as a tumor-treating field-sensitizer in colon cancer therapy. Cancers (Basel) 2019; 11: 1999.
[36] Chen Z, Cao K, Xia Y, Li Y, Hou Y, Wang L, Li L, Chang L and Li W. Cellular senescence in ionizing radiation (Review). Oncol Rep 2019; 42: 883-894.
[37] Tabasso AFS, Jones DJL, Jones GDD and Macip S. Radiotherapy-induced senescence and its effects on responses to treatment. Clin Oncol (R Coll Radiol) 2019; 31: 283-289.
[38] Lee JJ, Kim BC, Park MJ, Lee YS, Kim YN, Lee BL and Lee JS. PTEN status switches cell fate between premature senescence and apoptosis in glioma exposed to ionizing radiation. Cell Death Differ 2011; 18: 666-677.
[39] Rayess H, Wang MB and Srivatsan ES. Cellular senescence and tumor suppressor gene p16. Int J Cancer 2012; 130: 1715-1725.
[40] Mallette FA, Goumard S, Gaumont-Leclerc MF, Moiseeva O and Ferbeyre G. Human fibroblasts require the Rb family of tumor suppressors, but not p53, for PML-induced senescence. Oncogene 2004; 23: 91-99.
[41] Kim WY and Sharpless NE. The regulation of INK4/ARF in cancer and aging. Cell 2006; 127: 265-275.
[42] Herbig U, Jobling WA, Chen BP, Chen DJ and Sedivy JM. Telomere shortening triggers senescence of human cells through a pathway involving ATM, p53, and p21(CIP1), but not p16(INK4a). Mol Cell 2004; 14: 501-513.
[43] Kang C, Xu Q, Martin TD, Li MZ, Demaria M, Aron L, Lu T, Yankner BA, Campisi J and Elledge SJ. The DNA damage response induces inflammation and senescence by inhibiting autophagy of GATA4. Science 2015; 349: aaa5612.
[44] Thirukkumaran C, Shi ZQ, Thirukkumaran P, Luider J, Kopciuk K, Spurrell J, Elzinga K and Morris D. PUMA and NF-kB are cell signaling predictors of reovirus oncolysis of breast cancer. PLoS One 2017; 12: e0168233.
[45] Dhawan P, Su Y, Thu YM, Yu Y, Baugher P, Ellis DL, Sobolik-Delmaire T, Kelley M, Cheung TC,

Ware CF and Richmond A. The lymphotoxin-beta receptor is an upstream activator of NF-kappaB-mediated transcription in melanoma cells. J Biol Chem 2008; 283: 15399-15408.
[46] Luo H, Yang A, Schulte BA, Wargovich MJ and Wang GY. Resveratrol induces premature senescence in lung cancer cells via ROS-mediated DNA damage. PLoS One 2013; 8: e60065.
[47] Jo Y, Oh G, Gi Y, Sung H, Joo EB, Lee S and Yoon M. Tumor treating fields (TTF) treatment enhances radiation-induced apoptosis in pancreatic cancer cells. Int J Radiat Biol 2020; 96: 1528-1533.
[48] Hornsby PJ. Senescence as an anticancer mechanism. J Clin Oncol 2007; 25: 1852-1857.
[49] Cagnol S and Chambard JC. ERK and cell death: mechanisms of ERK-induced cell death--apoptosis, autophagy and senescence. FEBS J 2010; 277: 2-21.
[50] Yang D, Song J, Wu L, Ma Y, Song C, Dovat S, Nishizaki T and Liu J. Induction of senescence by adenosine suppressing the growth of lung cancer cells. Biochem Biophys Res Commun 2013; 440: 62-67.
[51] Shao M, Geng Y, Lu P, Xi Y, Wei S, Wang L, Fan Q and Ma W. Retraction notice to "miR-4295 promotes cell proliferation and invasion in anaplastic thyroid carcinoma via CDKN1A" [Biochem. Biophys. Res. Commun. 464/4 (2015) 1309-1313]. Biochem Biophys Res Commun 2019; 515: 728.
[52] Gewirtz DA, Holt SE and Elmore LW. Accelerated senescence: an emerging role in tumor cell response to chemotherapy and radiation. Biochem Pharmacol 2008; 76: 947-957.
[53] Acosta JC and Gil J. Senescence: a new weapon for cancer therapy. Trends Cell Biol 2012; 22: 211-219.
[54] Olivier M, Petitjean A, Marcel V, Petre A, Mounawar M, Plymoth A, de Fromentel CC and Hainaut P. Recent advances in p53 research: an interdisciplinary perspective. Cancer Gene Ther 2009; 16: 1-12.